Analytica Chimica Acta 1158 (2021) 338415

Contents lists available at ScienceDirect

Analytica Chimica Acta

journal homepage: www.elsevier.com/locate/aca

A novel miniaturized homogeneous label-free electrochemical biosensing platform combining integrated microelectrode and functional nucleic acids

Fangming Chen [a], Xingchuang Fu [a], Yao Meng [a], Mingrui Jiang [a], Jian Wang [a, b, **], Ying-Lin Zhou [c, ***], De-Wen Zhang [a, b, *]

[a] Institute of Medical Engineering, Department of Biophysics, School of Basic Medical Sciences, Health Science Center, Xi'an Jiaotong University, Xi'an, 710061, China
[b] Key Laboratory of Environment and Genes Related to Diseases, Xi'an Jiaotong University, Ministry of Education of China, Xi'an, 710061, China
[c] Beijing National Laboratory for Molecular Sciences (BNLMS), MOE Key Laboratory of Bioorganic Chemistry and Molecular Engineering, College of Chemistry and Molecular Engineering, Peking University, Beijing, 100871, China

HIGHLIGHTS

- Integrated microelectrode (IME) for electrochemical monitoring at microliter level
- The G3/MB complex was used as the signal generator in the electrochemical biosensor
- The poly T and G3 were designed into one single-stranded functional DNA hairpin
- Target induced conformation switching of DNA hairpin can release G3 part
- Homogeneous label-free electrochemical biosensing platform based on IME and G3/MB

GRAPHICAL ABSTRACT

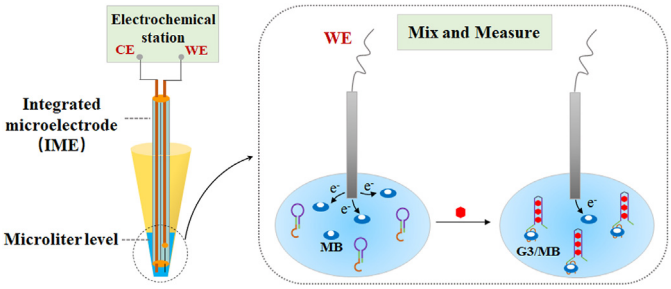

ARTICLE INFO

Article history:
Received 8 February 2021
Received in revised form
10 March 2021
Accepted 11 March 2021
Available online 17 March 2021

Keywords:
Integrated microelectrode

ABSTRACT

A miniaturized platform combining integrated microelectrode (IME) and functional nucleic acids was developed for homogeneous label-free electrochemical biosensing. IME was constructed with a carbon fiber microelectrode and a platinum wire in a θ type glass tube as a two-electrode system for electrochemical monitoring at microliter level. A newly reported G-triplex/methylene blue (G3/MB) complex was used as the signal generator in the homogeneous label-free electrochemical biosensor. G3 has strong affinity with MB and it can cause significant decrease of the diffusion current of MB after binding. Melamine was chosen as the model target. Since melamine can interact with nucleobase thymine (T) to form T-melamine-T structure through complementary hydrogen bonds, a single-strand functional DNA

* Corresponding author. Institute of Medical Engineering, Department of Biophysics, School of Basic Medical Sciences, Health Science Center, Xi'an Jiaotong University, Xi'an, 710061, China.
** Corresponding author. Institute of Medical Engineering, Department of Biophysics, School of Basic Medical Sciences, Health Science Center, Xi'an Jiaotong University, Xi'an, 710061, China.
*** Corresponding author.
E-mail addresses: jian.wang@xjtu.edu.cn (J. Wang), zhouyl@pku.edu.cn (Y.-L. Zhou), zhangdewen@xjtu.edu.cn (D.-W. Zhang).

https://doi.org/10.1016/j.aca.2021.338415

Homogeneous label-free
Biosensor
G-triplex
Methylene blue

hairpin structure with poly T and G3 elaborately blocked via base pairing was designed. The presence of melamine can trigger the conformation switching of the DNA hairpin to release the G3. The released G3 combined with MB could therefore change the diffusion current, leading to a simple and rapid detection of melamine. The combination of functional DNA hairpin as target recognition element, G3/MB as signal generator, and IME as transducer provided a "Mix and Measure" miniaturized platform for the construction of homogeneous label-free electrochemical biosensors.

1. Introduction

Electrochemical biosensors have gained tremendous attention over decades as a powerful analytical category [1,2]. Most of electrochemical biosensors are designed as heterogeneous assays with bio-recognition probe immobilized on the electrode surface [3,4]. Despite the high sensitivity, the heterogeneous detection takes the risk of biological activity loss or unsuccessful binding of bio-recognition probes [5,6]. The development of homogenous electrochemical biosensor can solve these problems with advantages of repeatability and being easy to operate after reducing the sample consumption to acceptable level. As the affinity reaction occurs in the solution rather than on the electrode-solution interface, there is no requirement for immobilization processes, which enables homogeneous electrochemical sensors to be cost-effective, reliable and easy-to-use [7–9].

As homogenous electrochemical biosensors are usually based on disposable reactions, keeping the sample consumption at microliter level is important in real biosensing applications. The previous work proposed a miniaturized device which set the electrochemical reaction in a micropipet tip assembled with a reproducible carbon ultramicroelectrode [10]. This device could significantly reduce the sample consumption, making the disposable homogeneous detection be affordable, which has been used for the development of homogeneous label-free electrochemical aptasensor [11] and DNAzyme biosensor [12]. However, the device used milliliter volume of supporting electrolyte assembled with conventional counter electrode and reference electrode to form a full three-electrode system, which increased the real size of the detection system. Moreover, it is limited by the detection time because of the slow diffusion between the analyte solution in micropipet tip and the outside supporting electrolyte, and thus eventually restricting the application scope of the device. To solve the problem, we developed a miniaturized electrochemical platform based on IME in this work by assembling a carbon fiber microelectrode as the working electrode and a platinum wire as the counter electrode into two separate channels of a θ type glass microtube, respectively (Fig. 1). Due to the small IR drop of microelectrode, a two-electrode system can be applied in the electrochemical detection [13]. The IME exhibited a similar electrochemical performance compared to the conventional three-electrode system but with a further compact and miniaturized setup, which allows it to be used for in-situ electrochemical detection in any small volume sample.

Among the homogeneous electrochemical biosensors, functional nucleic acid-based electrochemical strategy is one of major research focuses [14–17]. G-quadruplex DNA (G4) was widely applied as a signal readout element in the form of peroxidase-mimicking G4/hemin DNAzyme [18–20] and G4/MB interaction [21–23]. Recently, a new G-triplex DNA (G3) was reported to have stronger affinity with MB than G4. The formation of G3/MB complex could dramatically decrease the diffusion current of MB on the electrode surface [24], which can be readily adopted in the construction of homogeneous label-free electrochemical biosensors [25].

Herein, the combination of G3/MB with IME was developed for a miniaturized homogeneous label-free electrochemical biosensing platform. Melamine was chosen as a model target. Because of the high nitrogen level (66% nitrogen by mass), melamine was found to be illegally added into milk products as an unacceptable non-protein N source. Since melamine can interact with nucleobase thymine (T) through the formation of complementary hydrogen bonds to form T-melamine-T triplex structure [26–30], we designed a single-stranded functional nucleic acid (denoted as G3-polyT-P10) including G3 and poly T bases (Fig. 1). Initially, both of G3 and poly T were elaborately blocked through the hairpin structure with 10 base pairs. With the presence of melamine, the binding of melamine and T caused the conformation switching of the nucleic acid and resulted in the release of G3 part. As G3 has strong affinity with MB to form a stable G3/MB complex, the diffusion current of MB significantly decreased, which could be detected by IME at microliter sample level. Within the miniaturized platform, a simple and rapid "Mix and Measure" strategy was proposed and demonstrated, which has great potential to promote the development of homogeneous label-free electrochemical biosensing.

2. Experimental section

2.1. Chemicals

All DNA oligonucleotides were synthesized by Sangon Biological Engineering Technology & Services Co., Ltd. (Shanghai, China) and have the following sequences from the 5′ end to 3′end (the boldface portion is the G3 sequence):

CTGGGAGGGAGGGA, G3;

CTGGGAGGGAGGGA*AAATTTTTTTTTTTTTTCTTTTTTTTTTTTTTCCC*, G3-polyT-P7;

CTGGGAGGGAGGGA*AAAATTTTTTTTTTTTTTCTTTTTTTTTTTTTTCCC*, G3-polyT-P8;

CTGGGAGGGAGGGA*AAAAATTTTTTTTTTTTTTCTTTTTTTTTTTTTTCCC*, G3-polyT-P9;

CTGGGAGGGAGG-GA*AAAAAATTTTTTTTTTTTTTCTTTTTTTTTTTTTTCCC*, G3-polyT-P10;

CTGGGAGGGAGG-GA*AAAAAAATTTTTTTTTTTTTTCTTTTTTTTTTTTTTCCC*, G3-polyT-P11;

CTGGGAGGGAGG-GA*AAAAAAAATTTTTTTTTTTTTTCTTTTTTTTTTTTTTCCC*, G3-polyT-P12;

CTGGGAGGGAGG-GA*AAAAAAAAATTTTTTTTTTTTTTCTTTTTTTTTTTTTTCCC*, G3-polyT-P13.

Melamine was obtained from Aladdin (Shanghai, China). Methylene blue (MB) was purchased from Kermel (Tianjin, China). $K_3Fe(CN)_6$, $K_4Fe(CN)_6$, KCl and Tris base were purchased from the Sinopharm Chemical Reagent Co., Ltd (Shanghai, China). All oligonucleotides were dissolved in 10 mM pH 7.4 Tris-HCl buffer containing 0.1 M KCl. The Tris buffer was used for all of the experiments

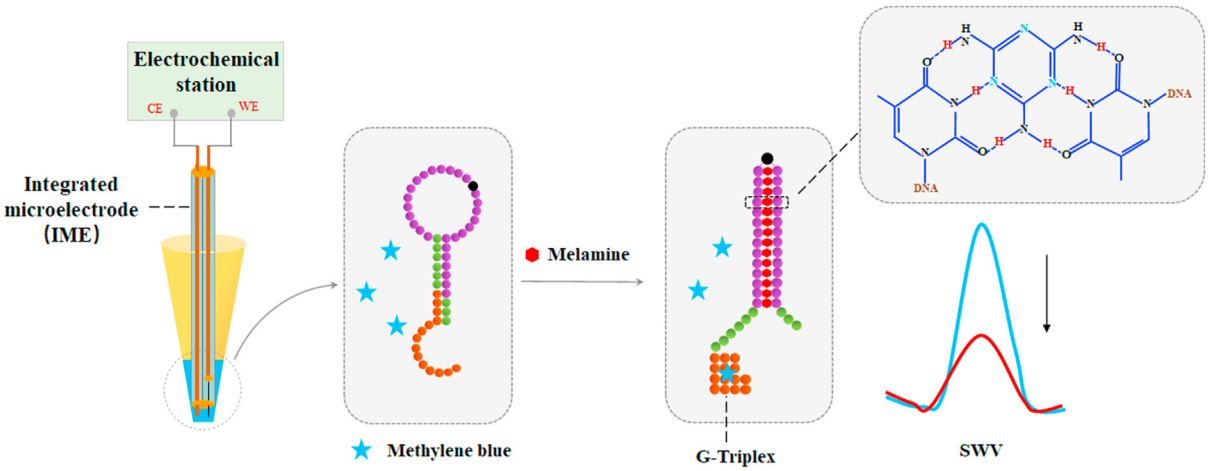

Fig. 1. Schematic diagram for G triplex-based functional DNA hairpin combined with IME for homogeneous label-free electrochemical biosensor.

unless specifically mentioned. All reagents were analytical reagents and prepared in ultrapure water obtained from a Milli-Q water purification system (Bedford, MA).

2.2. Fabrication of IME

Carbon fibers (7 μm diameter) were cleaned in an ultrasonic bath with acetone, ethanol, and ultrapure water for 10 min respectively and dried in air. Then the carbon fiber (1 cm length) was connected to a copper wire (400 μm diameter, 6 cm length) with conductive silver paint. This wire was inserted into one chamber of a θ type glass microtube (1.50 cm outer diameter, 1.17 cm inner diameter, 0.165 mm thickness of glass membrane, purchased from Sutter Instrument Company, USA) with a part of carbon fiber exposed outside, while a platinum wire (400 μm diameter, 6 cm length) was inserted into the other chamber with a part exposed outside. One end with carbon fiber and platinum wire of the θ type glass microtube was sealed with silicone rubber, the other end with copper wire and platinum wire was sealed with epoxy. Before use, the prepared IME was quickly swept over the outer flame of the alcohol lamp for cleaning of the carbon fiber. The schematic diagram of the IME was shown in Fig. 1. A scanning electron microscope (GeminiSEM 500, Germany) was used to characterize the tip of the prepared IME.

2.3. Electrochemical measurements

A CHI 660E electrochemical workstation (Shanghai Chenhua Instruments Co., Shanghai, China) was employed to perform the electrochemical experiments. As shown in Fig. 1, the IME was based on a two-electrode system using carbon fiber as the working electrode and platinum as the counter electrode. During measurements, the IME was inserted into a micropipet tip containing the analyte solution with a fixed 20 μL reaction volume for rapid and accurate mixture by the vortex. The cyclic voltammetry (CV) was measured at a scan range of −0.7–0.7 V and a scan rate of 0.1 V/s. The Square wave voltammetry (SWV) was recorded at a frequency of 50 Hz, a pulse amplitude of 50 mV with an incremental potential of 5 mV. Before electrochemical measurements, the nucleic acid G3-polyT-P10 dissolved in buffer solution was annealed using TC1000-G Gradient PCR (DLAB, Beijing, China). It was heated to 90 °C for 3 min, and then slowly cooled to 25 °C at 0.05 °C/s. For melamine sensing, different concentrations of melamine (100 μM-5 mM) were incubated with G3-polyT-P10 at 25 °C for 30 min.

3. Results and discussion

3.1. Fabrication and characterization of IME

Fig. 2A shows the zoomed optical image taken from the tip part of the prepared IME. And the SEM picture of the carbon fiber (7 μm diameter) part of the IME was shown in Fig. 2B. The carbon fiber was worked as the working electrode, while the Pt wire (400 μm diameter) was worked as the counter electrode. The electrode area of counter electrode was designed to be much larger than working electrode to avoid the interference of electrode polarization. A θ type glass microtube with two separate chambers was used to ensure there was no physical contact between the two electrodes. To validate the feasibility of IME for electrochemical measurements, a comparison of CV curves measured with IME and a traditional three-electrode system in 5 mM $K_3/K_4Fe(CN)_6$ solution was presented in Fig. 2C. The IME was inserted into a micropipet tip containing 20 μL measurement solution, while the traditional three-electrode system was performed in 5 mL 5 mM $K_3/K_4Fe(CN)_6$ solution using carbon fiber part of IME as the working electrode, an Ag/AgCl reference electrode and a Pt counter electrode. The results showed an analogous curve shape and the same quasi-steady state current only with a 215 mV voltage shift, indicating that the IME could perform similar electrochemical analysis at a microliter volume level as the three-electrode system. The volume of sample solution using IME could fall lowest to 1 μL. For convenience of quantitative mixture of sample solution by conventional vortex mixer, we chose 20 μL in the following experiments. The quasi-steady state current of IME for quantitative detections of redox substrate was investigated. For the columnar microelectrode, the quasi-steady state current accords with the equation $i_{qss} = (2nFAD_0C_0^*)/(r_0 \ln\tau)$, where C_0^* is the concentration of the electroactive species. The CV curves of $K_4Fe(CN)_6$ and dopamine with different concentrations were measured by the IME in a micropipet tip. The oxidation quasi-steady state currents were proportional to the concentration of the reductive substrate (Fig. 2 D and E). Rather than a typical quasi-steady state current-voltage curve, the CV curves of MB showed a pair of redox peaks correlated to its concentration, which is agreed with the previous report based on a carbon fiber ultramicroelectrode assembled in a three-electrode system [23]. The IME can be reused as a detector. In a group of experiments, it can be cleaned by rinsing with water or by

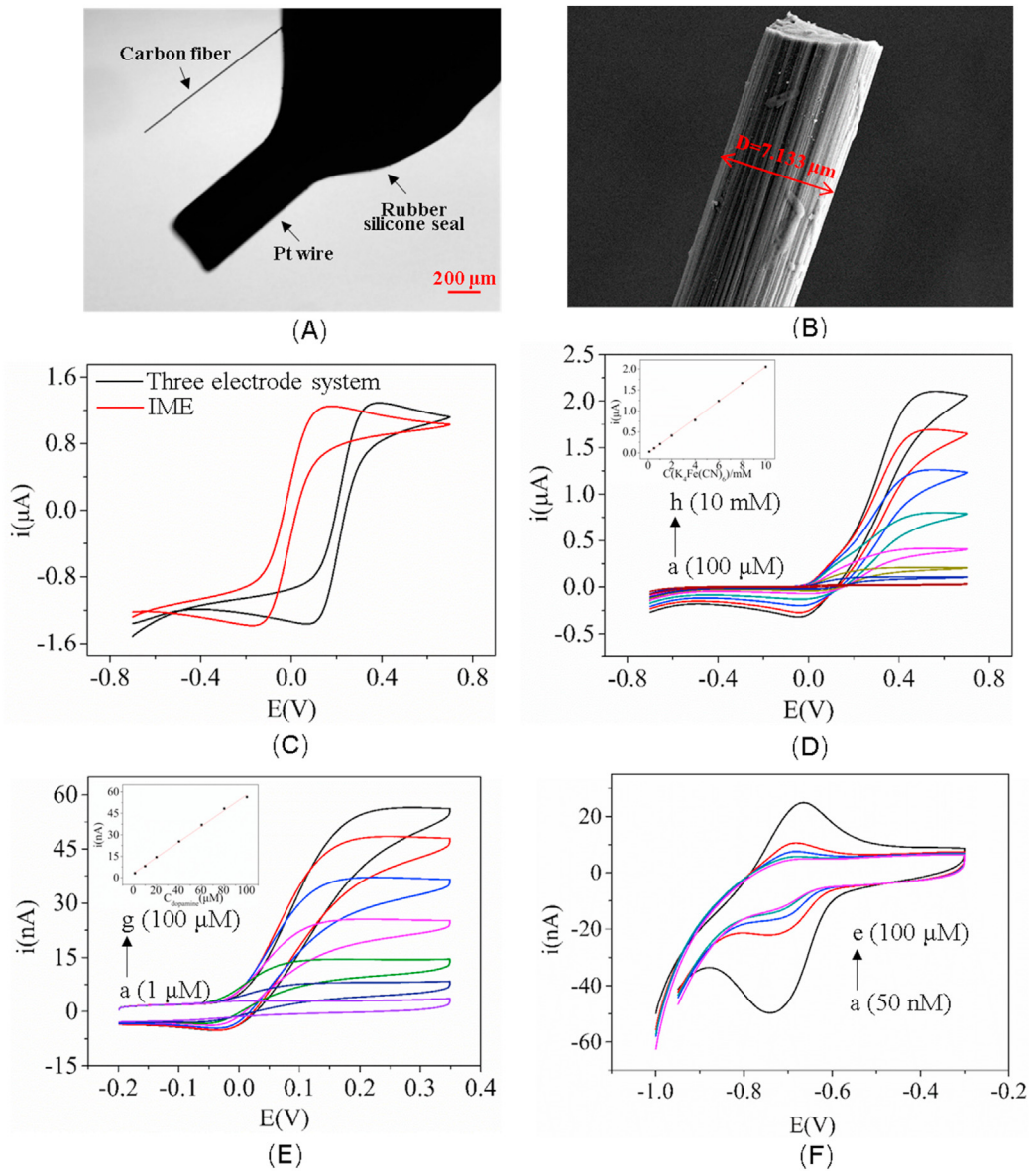

Fig. 2. (A) Optical micrograph taken from the tip part of the IME. (B) The SEM picture of the carbon fiber (7 μm diameter) part of the IME. (C) CV curves of IME and three-electrode system measured in 5 mM $K_3/K_4Fe(CN)_6$ solution. The IME was inserted into a micropipet tip containing 20 μL solution, while the three-electrode system was performed in 5 mL solution using carbon fiber part of IME as the working electrode, an Ag/AgCl reference electrode and a Pt counter electrode; (D) CV of 100 μM, 500 μM, 1 mM, 2 mM, 4 mM, 6 mM, 8 mM, 10 mM $K_4Fe(CN)_6$. (E) CV of 0, 10 μM, 20 μM, 40 μM, 60 μM, 80 μM, 100 μM dopamine. (F) CV of 50 nM, 500 nM, 1 μM, 10 μM, 100 μM MB.

ethanol immersion and then water immersion, which keeps the effective electrode area and electrochemical performance highly repeatable. If the electrode surface is contaminated and cannot be cleaned by water and ethanol, the IME can be flamed rapidly by an alcohol lamp to be cleaned completely, which make it as a new detector.

3.2. The affinity interaction of MB and G3

MB has been widely used as an electrochemical indicator. Fig. 3A shows the SWV curves of MB measured with IME. The peak current increased with the increasing of MB concentration from 0 μM to 10 μM, indicating a quantitative analysis based on MB can be achieved by using IME. G3 is a newly discovered DNA sequence which could form a stable complex with MB and cause a significant decrease of diffusion current of MB. In this work the G3/MB complex was adopted for the construction of homogeneous label free electrochemical assays. The interaction activity was demonstrated using IME based SWV measurements. As shown in Fig. 3B, due to the presence of G3, the peak current of MB decreased. And a higher concentration of G3 resulted in a lower current of MB until the G3 concentration was equal to the MB concentration (8 μM), which indicated that the combination ratio of G3 and MB was 1:1. The homogeneous electrochemical response of G3/MB interaction provided a promising signal generator in label-free biosensors based on functional nucleic acids.

3.3. Miniaturized platform for electrochemical biosensing of melamine

Melamine was chosen as the model target. Since it could specifically interact with T to form a DNA triplex, a ssDNA hairpin

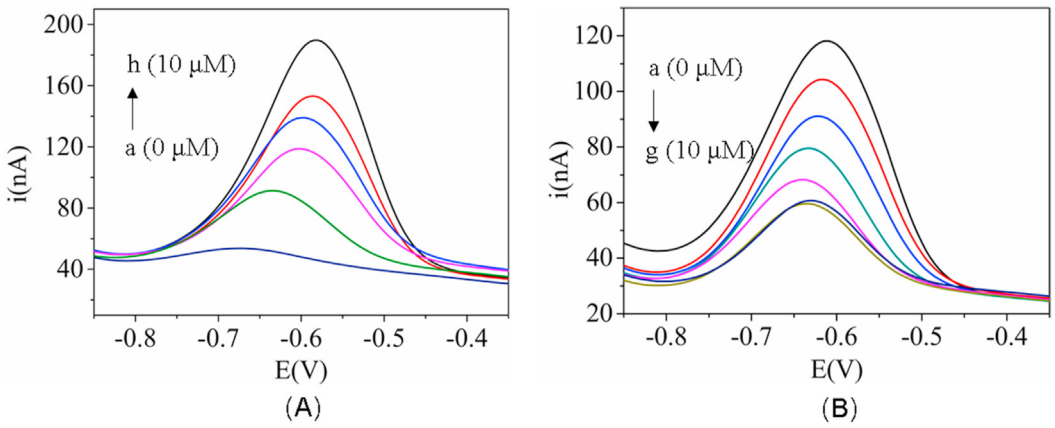

Fig. 3. (A) SWV of (a) 0 μM, (b) 2 μM, (c) 4 μM, (d) 6 μM, (e) 8 μM, (f) 10 μM MB. (B) SWV responses of 8 μM MB in the (a) absence and (b–g) presence of different G3 concentrations: 1, 2, 4, 6, 8, 10 μM.

structure (G3-polyT-P10) was designed, which comprised poly T (purple) in the loop and G3 (orange) the tail region (Fig. 1). Initially, the poly T and G3 were blocked by the stem structure of the hairpin. With the addition of melamine, the hairpin structure was opened due to the complementary hydrogen bonds of T-melamine-T triplex structure, triggering the release of the G3 sequence. G3 could therefore specifically bind with MB, resulting in a reduction of the diffusion current. Fig. 4A validates the feasibility of melamine sensing based on this strategy, which shows an obvious decrease of peak current as expected in the presence of melamine.

Experimental parameters including the reaction time, ratios of reactants and hairpin DNA sequence were investigated and optimized. To explore the optimal reaction time of G3-polyT-P10 and melamine, the SWV current of MB was continuously monitored after the addition of melamine. As shown in Fig. 4B, the SWV peak current of MB kept decrease until the reaction of melamine and hairpin reached equilibrium at around 30 min. The long-time monitoring of the system presented the advantage of the combination of IME and G3/MB in continuous detection in microliter volume sample. To ensure most of the hairpin was released by the interaction with melamine, 30 min was adopted as the incubation time in the following experiments.

The ratio of MB and hairpin was another important factor as the electrochemical signal was directly affected by their reaction

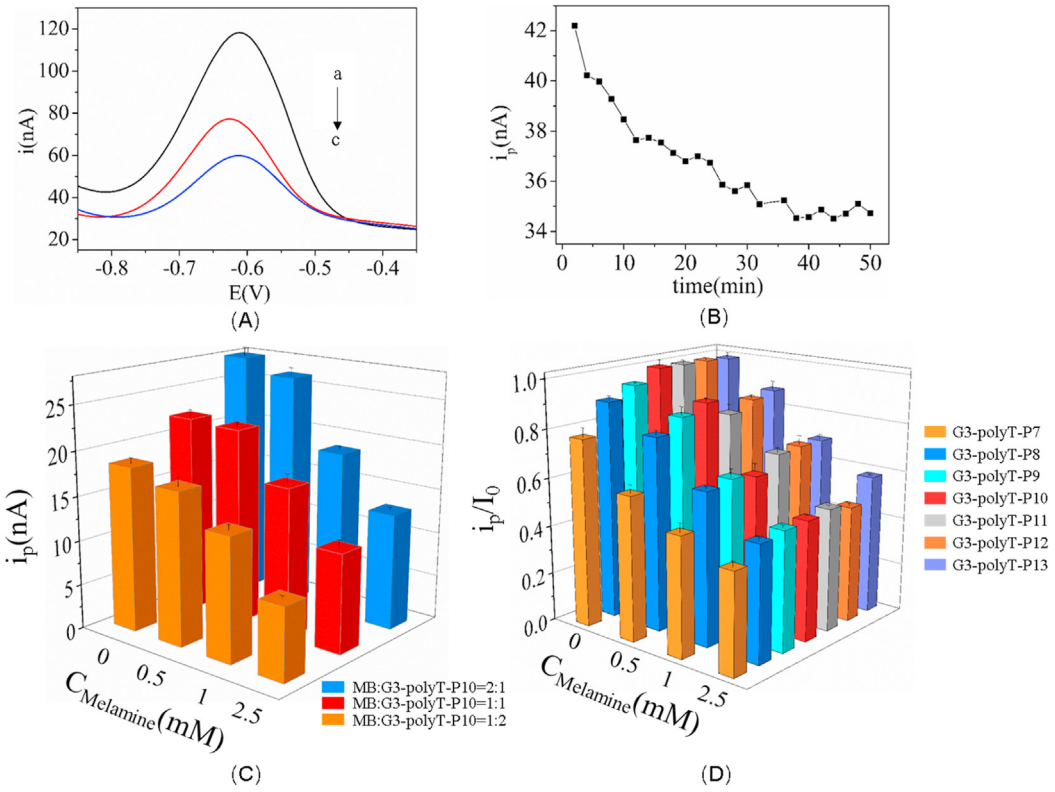

Fig. 4. (A) SWV of (a) 10 μM MB, (b) 10 μM MB and 5 μM G3-polyT-P10, (c) 10 μM MB, 5 μM G3-polyT-P10, and 1 mM melamine. Each curve was measured after 30 min incubation. Optimization of (B) the reaction time with 10 μM MB, 5 μM G3-polyT-P10 and 1 mM melamine, (C) the concentration ratio of MB to 5 μM G3-polyT-P10, and (D) the number of base pairs in stem complementary region of DNA hairpin.

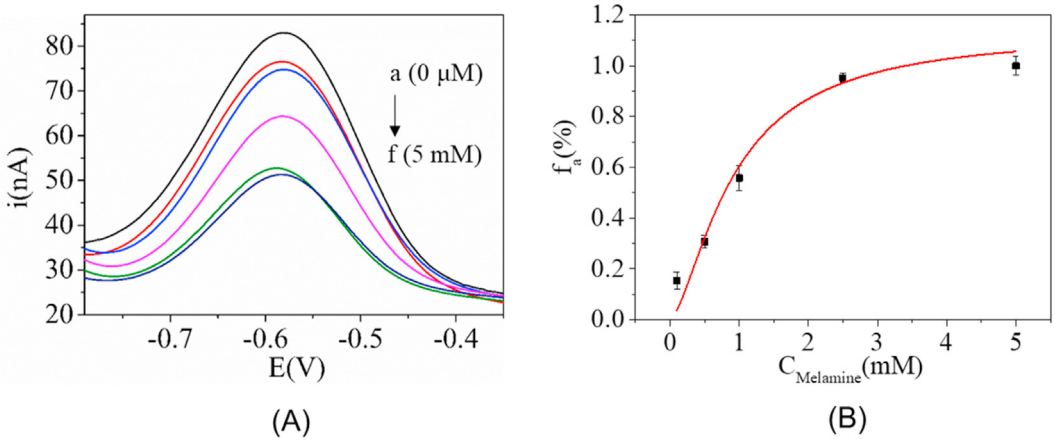

Fig. 5. (A) SWV of 10 μM MB and 5 μM G3-polyT-P10 in the (a) absence and (b–f) presence of different concentrations of melamine: 100 μM, 500 μM, 1 mM, 2.5 mM, 5 mM after incubating for 30 min. (B) The binding curves of the biosensor with concentrations of melamine, where f_a (%) is the fraction bound of DNA hairpin with melamine. The red curve is the fitting curve by the Hill equation ($R^2 = 0.96$). N = 3. (For interpretation of the references to colour in this figure legend, the reader is referred to the Web version of this article.)

efficiency. By fixing the concentration of G3-polyT-P10 to 5 μM, different ratios of MB: G3-polyT-P10 = 1:2; 1:1; 2:1 were used to detect melamine. As shown in Fig. 4C, the reduction of the diffusion current of MB was most significant when MB: G3-polyT-P10 = 2:1.

In our design, the poly T and G3 were initially blocked via hairpin. According to the end of G3 sequence (5′-CTGGGAGG-GAGGGA-3′), four bases "CCCT" in the 3′ end of the hairpin are chosen to cage "GGGA" unit of G3. Fixing four base pairs to block G3, then we choose suitable base pair number to block a part of polyT. To guarantee a sensitive triggering of target, the degree of blocking should be optimized by adjusting the base pair number of the stem duplex. It is believed that more complementary base pairs result in a higher thermodynamic stability of well-formed hairpin structure, leading the stronger blocking of G3 and the higher initial current. On the other side, more complementary base pairs of stem duplex are more difficult to be opened by the formation of T-melamine-T triplex, which means a lower signal change. The balance point of complementary base pairs needs to be investigated. A series of hairpins with different base pairs (denoted as G3-polyT-P7, G3-polyT-P8, G3-polyT-P9, G3-polyT-P10, G3-polyT-P11, G3-polyT-P12 and G3-polyT-P13) were employed to detect melamine. The secondary structures and free energy of the seven hairpins were evaluated by the OligoAnalyzer program (Integrated DNA Technologies, Inc. USA). As the base pair number increases from 7 to 13, free energy values are −3.6 kcal/mol, −4.7 kcal/mol, −5.9 kcal/mol, −7.0 kcal/mol, −8.1 kcal/mol, −9.2 kcal/mol, −10.3 kcal/mol, respectively. The theoretical data further supported the relationship between the base pair number and the thermodynamic stability of hairpin structure. All the current responses were normalized using the initial SWV current of G3-polyT-P10/MB as the standard unit for comparison. i_p/I_0 was defined as the ordinate of Fig. 4D, while I_0 is the initial SWV peak current of MB/G3-polyT-P10 in the absence of melamine. From the results shown in Fig. 4D, there was no apparent difference in terms of responses to the range of target concentrations in the groups of G3-polyT-P10, G3-polyT-P11, and G3-polyT-P12. When the base pairs were less than 10, a low thermodynamic stability of hairpin structure led to a low initial signal and thus the sensitivity for melamine detection at low concentration was reduced. In contrast, 13 base pairs can effectively block the G3 but the sensor response was also reduced due to the high stability of hairpin. Therefore, G3-polyT-P10 was chosen as the hairpin sequence in the study, which reduced the cost of synthesized DNA compared to G3-polyT-P11 and G3-polyT-P12.

The electrochemical biosensing of melamine was studied based on the optimized parameters. Melamine samples at different concentrations were mixed with annealed hairpin and MB to trigger the conformation switching. As illustrated in Fig. 5A, the SWV peak current gradually decreased with the increase of melamine concentration from 100 μM to 5 mM, which agreed with the principle that a higher concentration of melamine would induce more G3 release and form more G3/MB complex to reduce the diffusion current.

The miniaturized platform combining IME and G3/MB complex could be used for the investigation of the dissociation constant (K_d) in affinity reaction between functional nucleic acids and target molecule. The linear relationship between SWV peak current of IME and free MB concentration provided the basis of quantitative analysis. The combination ratio of G3 and MB that is 1:1 simplified the process of modeling and calculation. The concentration of DNA/Target complex is in direct proportion to the SWV peak current (i_p). The fraction bound of DNA (f_a) can be calculated as $f_a(\%) = \frac{[Complex]}{[DNA]} = \frac{I_0 - i_p}{I_0 - I_{min}}$, where I_0 is the initial SWV peak current in the absence of target melamine, I_{min} is the SWV peak current when the DNA/melamine complex reached saturation in the homogeneous solution.

As mentioned above and Fig. 1, there are multiple binding sites of melamine within a functional DNA containing poly T. Therefore, an apparent constant $K_{1/2}$, which is the target concentration at which on-half of the receptor binding sites are occupied [30], was used for characterization of affinity between DNA and target melamine instead of K_d. The binding curve with melamine concentration is well fitted by the Hill equation with Hill coefficients.

$$f_a(\%) = \frac{[target]^{n_H}}{[target]^{n_H} + K_{1/2}{}^{n_H}}$$

where [target] is the concentration of uncombined melamine. As the concentration of melamine is much higher than the DNA hairpin G3-polyT-P10, it can be directly used for the fitting of the binding curve. Fig. 5 B shows the fitting curve ranging from 100 μM to 5 mM with a Hill coefficient of 1.5 and $K_{1/2}$ of about 920 μM ($R^2 = 0.96$). It shows the detection range of melamine from 100 μM to 2.5 mM with the limit of detection (LOD) estimated to be 100 μM based on a signal-to-noise ratio (S/N) of 3.

The specificity of this assay was investigated by detecting dicyandiamide which shares the similar structure with melamine [27]. The results in Fig. 6 showed that 1 mM dicyandiamide caused

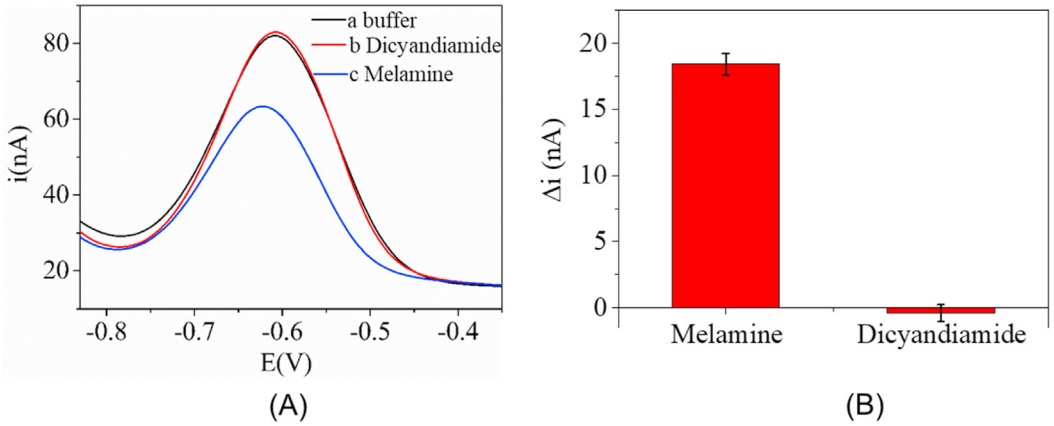

Fig. 6. (A) SWV of 10 μM MB and 5 μM G3-polyT-P10 in the (a) absence, presence of (b) 1 mM dicyandiamide and (c) 1 mM melamine after incubating for 30 min. (B) The SWV peak current change ($\Delta i = i_0 - i_p$) in the presence of melamine and dicyandiamide, n = 3.

Table 1
The rate of recovery detection of 1 mM melamine in milk sample.

	Detection in buffer Δi_{buffer} (nA)	Detection in milk sample $\Delta i_{milk\ sample}$ (nA)	Rate of recovery $\Delta i_{milk\ sample}/\Delta i_{buffer}$ (%)
$C_{Melamine}$ = 1 mM	23.7 ± 0.5	21.4 ± 1.1	90.3 ± 5.3

almost no change of the diffusion current of MB, while about 18.4 nA decrease of peak current was observed for melamine, indicating the good selectivity of the proposed biosensor.

An application of the proposed homogeneous label-free electrochemical biosensor in real samples was performed by measuring the commercially available infant formula powder adulterated with melamine. The milk powder mixed with melamine was dissolved in Tris buffer following the milk formula concentration. The blend was boiled for 10 min and filtered by a 0.2 μm filter to exclude the protein in milk. Prior assay the blend was diluted 10 times with the Tris buffer and the final concentration of melamine was 1 mM. One IME was used to keep the consistent senor performance. SWV of G3-polyT-P10/MB was measured in the Tris buffer, and the peak current was defined as i_0. Δi_{buffer} was the SWV peak current change ($\Delta i = i_0 - i_p$) in the presence of 1 mM melamine in the Tris buffer, while $\Delta i_{milk\ sample}$ was that in the presence of 1 mM melamine in diluted milk sample with the Tris buffer. The values were shown in Table 1. The recovery rate $\Delta i_{milk\ sample}/\Delta i_{buffer}$ was calculated as 90.3 ± 5.3%. It showed slight signal suppression in milk sample when compared with that in the Tris buffer, which was acceptable. This result suggested that this proposed biosensor based on IME and functional nucleic acids is promising for real samples.

4. Conclusion

In summary, we developed a miniaturized platform based on IME in combination with functional nucleic acids and G3/MB for homogeneous label-free electrochemical biosensing. As melamine was chosen to be the target model, a functional DNA hairpin structure consisted of poly T and G3 was designed for smart target triggering. The alteration of electrochemical signals resulted from the binding of G3 with MB was detected using IME. The IME featured with a two-electrode system requires microliter sample consumption, making the disposable homogeneous detection be affordable. The electrochemical measurement results showed that the sensor response to melamine ranging from 100 μM to 2.5 mM could be detected with high selectivity. And the miniaturized platform can be easily applied for the investigation of the dissociation constant in affinity reaction between functional nucleic acid and target molecule. Since the whole strategy is on basis of a simple "Mix and Measure" procedure without any complicated operation, this proposed biosensor has a great potential in the application of in-field electrochemical analysis and detection. If the electron transfer rate can be enhanced by changing the microelectrode material or surface modification, it is hopeful to improve the detection limit of MB and further improve the sensor performance.

CRediT authorship contribution statement

Fangming Chen: Data curation, Methodology, Writing – original draft. **Xingchuang Fu:** Data curation, Formal analysis, Resources. **Yao Meng:** Methodology. **Mingrui Jiang:** Methodology. **Jian Wang:** Conceptualization, Investigation, Supervision, Writing – review & editing, Funding acquisition. **Ying-Lin Zhou:** Supervision, Writing – review & editing. **De-Wen Zhang:** Conceptualization, Formal analysis, Project administration, Supervision, Writing – review & editing, Funding acquisition.

Declaration of competing interest

The authors declare that they have no known competing financial interests or personal relationships that could have appeared to influence the work reported in this paper.

Acknowledgments

This work was supported by the National Natural Science Foundation of China (Grant No. 22074116, 31800827), and the Fundamental Research Funds for the Central Universities (Grant No. xzy012019071).

References

[1] G. Maduraiveeran, M. Sasidharan, V. Ganesan, Electrochemical sensor and biosensor platforms based on advanced nanomaterials for biological and

biomedical applications, Biosens. Bioelectron. 103 (2018) 113–129.
[2] M. Trotter, N. Borst, R. Thewes, F. von Stetten, Review: electrochemical DNA sensing - principles, commercial systems, and applications, Biosens. Bioelectron. 154 (2020) 11.
[3] H. Li, P. Dauphin-Ducharme, N. Arroyo-Currás, C.H. Tran, P.A. Vieira, S. Li, C. Shin, J. Somerson, T.E. Kippin, K.W. Plaxco, A biomimetic phosphatidylcholine-terminated monolayer greatly improves the in vivo performance of electrochemical aptamer-based sensors, Angew. Chem. Int. Ed. 56 (2017) 7492–7495.
[4] M. Zhu, S. Li, H. Li, H. Li, F. Xia, employing an intercalated redox reporter in electrochemical aptamer-based biosensors to enable calibration-free molecular measurements in undiluted serum, Anal. Chem. 92 (2020) 12437–12441.
[5] X.L. Huang, Y.J. Liu, B. Yung, Y.H. Xiong, X.Y. Chen, Nanotechnology-enhanced No-wash biosensors for in vitro diagnostics of cancer, ACS Nano 11 (2017) 5238–5292.
[6] G.J. Han, Z. Xing, Y.H. Dong, S.C. Zhang, X.R. Zhang, One-step homogeneous DNA assay with single-nanoparticle detection, Angew. Chem. Int. Ed. 50 (2011) 3462–3465.
[7] T. Hou, N.N. Xu, W.X. Wang, L. Ge, F. Li, Label-free and immobilization-free photoelectrochemical biosensing strategy using methylene blue in homogeneous solution as signal probe for facile DNA methyltransferase activity assay, Biosens. Bioelectron. 141 (2019) 6.
[8] X.J. Liu, M.M. Song, T. Hou, F. Li, Label-free homogeneous electroanalytical platform for pesticide detection based on acetylcholinesterase-mediated dna conformational switch integrated with rolling circle amplification, ACS Sens. 2 (2017) 562–568.
[9] F.T. Zhang, L.Y. Cai, Y.L. Zhou, X.X. Zhang, Immobilization-free DNA-based homogeneous electrochemical biosensors, Trac-Trends Anal. Chem. 85 (2016) 17–32.
[10] D.W. Zhang, J.X. Liu, J. Nie, Y.L. Zhou, X.X. Zhang, Micropipet tip-based miniaturized electrochemical device combined with ultramicroelectrode and its application in immobilization-free enzyme biosensor, Anal. Chem. 85 (2013) 2032–2036.
[11] D.W. Zhang, J. Nie, F.T. Zhang, L. Xu, Y.L. Zhou, X.X. Zhang, Novel homogeneous label-free electrochemical aptasensor based on functional DNA hairpin for target detection, Anal. Chem. 85 (2013) 9378–9382.
[12] S.B. Xie, W. Yuan, P. Wang, Y. Tang, L.M. Teng, Q. Peng, Target-induced conformational switch of DNAzyme for homogeneous electrochemical detection of nereistoxin-related insecticide on an ultramicroelectrode, Sens. Actuator B-Chem. 292 (2019) 64–69.
[13] F.X. Chang, X. Xie, M.X. Li, Z.W. Zhu, A miniaturized electrochemical device integrating a biconical microchannel and carbon fiber disk ultramicroelectrode, Analyst 141 (2016) 4859–4862.
[14] H. Fu, C. Ge, W. Cheng, C.H. Luo, D.C. Zhang, L. Yan, Y. He, G. Yi, A hairpin electrochemical aptasensor for sensitive and specific detection of thrombin based on homogenous target recognition, Electroanalysis 25 (2013) 1223–1229.
[15] L.R. Schoukroun-Barnes, E.P. Glaser, R.J. White, Heterogeneous electrochemical aptamer-based sensor surfaces for controlled sensor response, Langmuir 31 (2015) 6563–6569.
[16] J. Wu, W. Lv, Q. Yang, H. Li, F. Li, Label-free homogeneous electrochemical detection of MicroRNA based on target-induced anti-shielding against the catalytic activity of two-dimension nanozyme, Biosens. Bioelectron. 171 (2021) 112707.
[17] X. Hai, Y. Li, C. Zhu, W. Song, J. Cao, S. Bi, DNA-based label-free electrochemical biosensors: from principles to applications, Trac-Trends Anal. Chem. 133 (2020) 116098.
[18] S. Chen, P. Liu, K.W. Su, X. Li, Z. Qin, W. Xu, J. Chen, C.R. Li, J.F. Qiu, Electrochemical aptasensor for thrombin using co-catalysis of hemin/G-quadruplex DNAzyme and octahedral Cu2O-Au nanocomposites for signal amplification, Biosens. Bioelectron. 99 (2018) 338–345.
[19] K.Y. Goud, K.K. Reddy, M. Satyanarayana, S. Kummari, K.V. Gobi, A review on recent developments in optical and electrochemical aptamer-based assays for mycotoxins using advanced nanomaterials, Microchim. Acta 187 (2019) 29.
[20] H. Chen, X. Sun, R. Cai, Y. Tian, N. Zhou, Switchable DNA tweezer and G-quadruplex nanostructures for ultrasensitive voltammetric determination of the K-ras gene fragment, Microchim. Acta 186 (2019) 843.
[21] D.L. Ma, Z.H. Zhang, M.D. Wang, L.H. Lu, H.J. Zhong, C.H. Leung, Recent developments in G-quadruplex probes, Chem. Biol. 22 (2015) 812–828.
[22] T. Cao, F.T. Zhang, L.Y. Cai, Y.L. Zhou, N.J. Buurma, X.X. Zhang, Investigation of the interactions between methylene blue and intramolecular G-quadruplexes: an explicit distinction in electrochemical behavior, Analyst 142 (2017) 987–993.
[23] F.T. Zhang, J. Nie, D.W. Zhang, J.T. Chen, Y.L. Zhou, X.X. Zhang, Methylene blue as a G-quadruplex binding probe for label-free homogeneous electrochemical biosensing, Anal. Chem. 86 (2014) 9489–9495.
[24] L.L. Zhao, T. Cao, Q.Y. Zhou, X.H. Zhang, Y.L. Zhou, L.J. Yang, X.X. Zhang, The exploration of a new stable G-triplex DNA and its novel function in electrochemical biosensing, Anal. Chem. 91 (2019) 10731–10737.
[25] L.L. Zhao, H.Y. Pan, X.X. Zhang, Y.L. Zhou, Ultrasensitive detection of microRNA based on a homogeneous label-free electrochemical platform using G-triplex/methylene blue as a signal generator, Anal. Chim. Acta 1116 (2020) 62–69.
[26] Y.Y. Zeng, Y. Pratumyot, X.J. Piao, D. Bong, Discrete assembly of synthetic peptide-dna triplex structures from polyvalent melamine-thymine bifacial recognition, J. Am. Chem. Soc. 134 (2012) 832–835.
[27] R.F. Su, H.R. Zheng, S.Y. Dong, R. Sun, S.N. Qiao, H.J. Sun, X.Y. Ma, T.H. Zhang, C.Y. Sun, Facile detection of melamine by a FAM-aptamer-G-quadruplex construct, Anal. Bioanal. Chem. 411 (2019) 10.
[28] K.L. Ai, Y.L. Liu, L.H. Lu, Hydrogen-bonding recognition-induced color change of gold nanoparticles for visual detection of melamine in raw milk and infant formula, J. Am. Chem. Soc. 131 (2009) 9496–9497.
[29] H. Huang, L. Li, G.H. Zhou, Z.H. Liu, Q. Ma, Y.Q. Feng, G.P. Zeng, P. Tinnefeld, Z.K. He, Visual detection of melamine in milk samples based on label-free and labeled gold nanoparticles, Talanta 85 (2011) 1013–1019.
[30] H. Li, J. Somerson, F. Xia, K.W. Plaxco, Electrochemical DNA-based sensors for molecular quality control: continuous, real-time melamine detection in flowing whole milk, Anal. Chem. 90 (2018) 10641–10645.